Received: 17 April 2018 | Revised: 30 June 2018 | Accepted: 6 July 2018

DOI: 10.1111/cas.13734

ORIGINAL ARTICLE

WILEY Cancer Science

Double-negative feedback interaction between DNA methyltransferase 3A and microRNA-145 in the Warburg effect of ovarian cancer cells

Songlin Zhang[1] | Meili Pei[2] | Zhen Li[2] | Han Li[2] | Yanli Liu[2] | Jie Li[2]

[1]Department of Structural Heart Disease, The First Affiliated Hospital of Xi'an Jiaotong University, Xi'an, China

[2]Department of Gynecology and Obstetrics, The First Affiliated Hospital of Xi'an Jiaotong University, Xi'an, China

Correspondence: Jie Li, Department of Gynecology and Obstetrics, The First Affiliated Hospital of Xi'an Jiaotong University, 277 West Yanta Road, Xi'an, Shaanxi 710061, China (lijiexj64@126.com).

Funding information
National Natural Science Foundation of China (No. 81702577).

Ovarian cancer is the most lethal gynecological malignancy because of its poor prognosis. The Warburg effect is one of the key mechanisms mediating cancer progression. Molecules targeting the Warburg effect are therefore of significant therapeutic value for the treatment of cancers. Many microRNAs (miR) are dysregulated in cancers, and aberrant miR expression patterns have been suggested to correlate with the Warburg effect in cancer cells. In our study, we found that miR-145 negatively correlated with DNA methyltransferase (DNMT)3A expression at cellular/histological levels. miR-145 inhibited the Warburg effect by targeting HK2. Luciferase reporter assays confirmed that miR-145-mediated downregulation of DNMT3A occurred through direct targeting of its mRNA 3′-UTRs, whereas methylation-specific PCR (MSP) assays found that knockdown of DNMT3A increased mRNA level of miR-145 and decreased methylation levels of promoter regions in the miR-145 precursor gene, thus suggesting a crucial crosstalk between miR-145 and DNMT3A by a double-negative feedback loop. DNMT3A promoted the Warburg effect through miR-145. Coimmunoprecipitation assays confirmed no direct binding between DNMT3A and HK2. In conclusion, a feedback loop between miR-145 and DNMT3A is a potent signature for the Warburg effect in ovarian cancer, promising a potential target for improved anticancer treatment.

KEYWORDS
DNMT3A, methylation, miR-145, ovarian cancer, the Warburg effect

1 | INTRODUCTION

Ovarian cancer is the most lethal gynecological malignancy, existing predominantly in the form of epithelial ovarian cancer (EOC).[1,2] EOC is the most common type of ovarian cancer and ranks as the seventh leading cause of cancer-related death in women.[3,4] Despite the use of aggressive treatments, most patients with EOC develop recurrent cancer; cancer metastasis is one of the leading causes of death.

The Warburg effect, which was first described by Warburg in the 1930s, is a metabolic reprogramming process used by cancer cells to support their high-energy requirements and high rates of macromolecular synthesis.[5,6] Several glycolytic enzymes control the Warburg effect, including hexokinase-2 (HK2), pyruvate kinase M2 (PKM2), pyruvate dehydrogenase kinase-1 (PDK-1), and lactate dehydrogenase (LDH). Of note, HK2 catalyzes the essentially irreversible first step of the glycolytic pathway in which glucose is phosphorylated to glucose-6-phosphate with concomitant dephosphorylation of ATP.[7] High expression and activity of these molecules in cancer cells lead to the high rates of glucose catabolism and lactate production that define the Warburg effect.

DNA methylation is a major epigenetic rule controlling chromosomal stability and gene expression,[8,9] which is controlled by DNA methyltransferases (DNMT). DNMT3A and DNMT3B are responsible for de novo methylation in the genome,[10] whereas DNMT1 is responsible for maintaining methylation in the genome. DNMT3A and DNMT3B have been reported to be upregulated in ovarian cancers.[11] They are both able to hypermethylate the promoter region in microRNA (miR) precursor genes and thus inversely regulate miR transcription.[9]

miR are small, noncoding RNAs that modulate gene expression at the post-transcriptional level through complementary binding to the 3′UTRs of target mRNAs.[12] miR-145 is shown to be downregulated in many cancers;[13-18] it functions as a tumor suppressor to inhibit tumor cell growth and survival, induce cell apoptosis and cell cycle arrest, and attenuate tumor cell migration and invasion by targeting various molecules.[14-16,19-22] In our study, we found that miR-145 inhibited aerobic glycolysis through directly targeting HK2. Using MethPrimer (http://www.urogene.org/methprimer/), we predicted that there were many methylations of CpG islands in the 5′ regulatory region of miR-145-5p. We propose that miR-145 expression is regulated by methylation.

Until now, the role of DNMT3A in cancer has been less studied than that of DNMT3B. Reports have shown that DNMT3A deficiency promotes tumor growth and progression.[10] However, few studies have been carried out to elaborate the role of DNMT3A in the Warburg effect. Herein, we report the interaction between miR-145 and DNMT3A and its underlying molecular mechanism in the Warburg effect in ovarian cancer cells in order to broaden our theoretical understanding of human ovarian cancer and to provide novel possibilities for future EOC treatment approaches.

2 | MATERIALS AND METHODS

2.1 | Human tissue specimens

Human ovarian carcinomas and normal ovarian tissue samples were collected from patients at The First Affiliated Hospital of Xi'an Jiaotong University, China. This study was approved by the Ethics Committee of The First Affiliated Hospital of Xi'an Jiaotong University, China. Written consent was obtained from each study participant enrolled. Clinicopathological characteristics of the informative cases are shown in Table 1.

2.2 | Cell culture and treatment with 5-aza-2′-deoxycytidine

The human ovarian cancer cell line SKOV3 was obtained from the Shanghai Cell Bank of Chinese Academy of Sciences (Shanghai, China); 3AO was obtained from the Shandong Academy of Medical Sciences (Jinan, China). Cells were maintained in RPMI 1640 medium (Gibco-BRL, Gaithersburg, MD, USA) supplemented with 10% (v/v) FBS at 37°C under a humidified 5% CO_2 atmosphere. Cells were allowed to attach for 4 or 5 days and treated with 0, 1 and 5 μmol/L 5-aza-2′-deoxycytidine (5-aza-CdR), respectively.

TABLE 1 Summary of clinical characteristics of patients in the present study

Characteristic	Cases
Ovarian cancer tissue	
Total number	31
Median age, years (range)	62 (43-75)
FIGO stage	
I/II	12
III/IV	19
Subtypes of ovarian cancer	
Serous cancer	19
Mucinous	9
Endometrioid cancer	1
Clear cell cancer	2
Normal ovarian tissue	
Total number	15

FIGO, International Federation of Gynecology and Obstetrics.

2.3 | Quantitative real-time PCR

Total RNA was extracted from cells using TRIzol reagent (Invitrogen, Carlsbad, CA, USA) according to the manufacturer's instructions. For mRNA detection, first-strand cDNA was synthesized using a RevertAid first-strand cDNA synthesis Kit (Thermo Fisher Scientific Inc., Waltham, MA, USA). qRT-PCR was carried out using a SYBR Premix Ex Taq II kit (Takara, Dalian, China) on a CFX96 real-time PCR system (Bio-Rad, Hercules, CA, USA). miR-145 was normalized to small nuclear U6, whereas HK2, LDH, PKM2, PFK2, PDK1 and DNMT3A were normalized to the gene β-actin. Relative gene expression was calculated automatically using $2^{-\Delta\Delta Ct}$. The following primer sequences were used.

DNMT3A forward: 5′- TATTGATGAGCGCACAAGAGAGC-3′;
DNMT3A reverse: 5′- GGGTGTTCCAGGGTAACATTGAG-3′;
HK2 forward: 5′- AAGGCTTCAAGGCATCTG-3′;
HK2 reverse: 5′ - CCACAGGTCATCATAGTTCC-3′;
LDH forward: 5′- GGCCTGTGCCATCAGTATCT-3′;
LDH reverse: 5′- GGAGATCCATCATCTCTCCC-3′;
PKM2 forward: 5′- TCCGGATCTCTTCGTCTTTG-3′;
PKM2 reverse: 5′- GTCTGAATGAAGGCAGTCCC-3′;
PFK2 forward: 5′- GCTATGAAACCAAAACCCCA-3′;
PFK2 reverse: 5′- TAACGATCAGAGTCGGGGAG-3′;
PDK1 forward: 5′- CAACAGAGGTGTTTACCCCC-3′;
PDK1 reverse: 5′- ATTTTCCTCAAAGGAACGCC-3′;
β-actin forward: 5′-TCCCTGGAGAAGAGCTACGA-3′;
β-actin reverse: 5′-AGCACTGTGTTGGCGTACAG-3′.

2.4 | Western blot

Total protein was collected from cells by RIPA lysis buffer containing protease inhibitors (Roche, Indianapolis, IN, USA) and 1 mmol/L

PMSF on ice. Protein concentration was measured using the BCA-200 Protein Assay kit (Pierce, Rockford, IL, USA). After heat denaturation at 100°C for 5 minutes, proteins were separated by electrophoresis on 10% SDS-PAGE gels and then transferred onto nitrocellulose membranes (Pall Life Science, Port Washington, NY, USA). The membranes were blocked with 5% nonfat milk at room temperature for 1 hour and then incubated overnight at 4°C with rabbit anti-human DNMT3A (1:500; Cell Signaling Technology, Danvers, MA, USA), HK2 (1:500; Cell Signaling Technology) and mouse anti-human β-actin (1:1000; Cell Signaling Technology). We increased the concentration of rabbit anti-human DNMT3A to 1:300 when the bands of DNMT3A were unclear. After washing with TBST, the blots were incubated with HRP-conjugated goat anti-rabbit or anti-mouse IgG. Blots were visualized using ECL reagents (Pierce, Rockford, IL, USA) by a chemiluminescence imaging system (Bio-Rad, Richmond, CA, USA).

2.5 | Plasmid transfection

Human DNMT3A expression vector pcDNA3/Myc-DNMT3A and HK2 expression vector PLHKII-pGFPN3 were obtained from Addgene (Boston, MA, USA). SKOV3 and 3AO cells were seeded into 6-well plates until 70%-90% confluency and transiently transfected with vector pcDNA3/Myc-DNMT3A(PLHKII-pGFPN3) or empty vector using the X-treme GENE HP DNA Transfection Reagent (Roche) following the manufacturer's protocol. After 48 hours of transfection, the cells were harvested for further study.

2.6 | Small interfering RNA and transient transfection

Human DNMT3A siRNA was purchased from GenePharma (Shanghai, China). Ovarian cancer cells were seeded into 6-well plates until they reached 40%-50% confluency. DNMT3A siRNA (CAGUGGUGUGUUGAGAATT) was transiently transfected 100 nmol/L per well using the X-treme GENE siRNA Transfection Reagent (Roche). After 48 hours transfection, the cells were harvested for further studies.

2.7 | Micro RNA transient transfection

Micro RNA-145 mimic and negative control were purchased from RiboBio Co. Ltd (Guangzhou, China). SKOV3 and 3AO cells were transiently transfected with 60 nmol/L miR-145 mimic or negative control using the X-treme GENE siRNA Transfection Reagent (Roche) following the manufacturer's protocol.

2.8 | Glucose consumption and lactate production assay

To determine the levels of glucose and lactate, supernatants of cell culture media were collected and detected using a glucose and lactate assay kit (BioVision, Milpitas, CA, USA) according to the manufacturer's instructions. Glucose consumption and lactate production were calculated based on the standard curve and normalized to the cell number.

2.9 | DNA bisulfite modification and methylation-specific PCR

Cells transfected by vector pcDNA3/Myc-DNMT3A for 48 hours in 24-well plates were trypsinized and resuspended in cold PBS at a concentration of ~6×10^6/mL. DNA bisulfite modification and purification were carried out using an EZ DNA methylation-Direct kit (Zymo Research, Irvine, CA, USA) according to the manufacturer's instructions. Concentration of DNA was evaluated by absorbance at 260 nm on a UV spectrophotometer (Bio-Rad Inc., Hercules, CA, USA).

The set of primers for methylation-specific PCR (MSP) was flanking the 3 kb 5′-region upstream from the start of the pre-miR-145 sequence. The primers for methylation-specific PCR were designed by MethPrimer, and the sequences were as follows: methylated (M)-forward (F): 5′-GGAGATTGGGGAATATATATGAGTC-3′; methylated (M)-reverse (R): 5′-AAAATAAAATACCACACGTCGC-3′; unmethylated (U)- forward (F): 5′-AGATTGGGGAATATATATGAGTTGT-3′; unmethylated (U)- reverse (R): 5′-ACCAAAATAAAATACCACACATCAC-3′. DNA amplification was carried out with Epi Taq HS (Takara) under the following conditions: 94°C for 5 minutes; 30 cycles of 94°C for 30 seconds, 50°C for 30 seconds, 72°C for 30 seconds; and 72°C for 10 minutes. The PCR productions were separated by 2.0% agarose gel electrophoresis and visualized by a chemiluminescence imaging system (Bio-Rad, Richmond, CA, USA).

2.10 | Luciferase reporter plasmid construction

Wild-type 3′-UTR sequences of the target genes carrying a putative miR-145 binding site were amplified by PCR. To generate mutant 3′-UTR fragments of miR-145 target genes, we adopted the two-step PCR method as reported previously. Briefly, two fragments of 3′-UTR were amplified by two sets of overlapped primers in which mutated seeding sequences of miR-145 were introduced. The wild-type and mutant PCR products were digested with *Hin*dIII and *Mlu*I enzymes, inserted into pMIR-REPORT Luciferase vectors (Ambion, Austin, TX, USA) and verified by DNA sequencing.

2.11 | Luciferase reporter assay

Cells were cotransfected with pRL-TK vector (20 ng), wild-type (WT-3′ UTR) or mutant (MUT-3′ UTR) reporter vectors (180 ng), along with miR-145 mimic or negative control at a final concentration of 20 nmol/L using the X-treme GENE siRNA Transfection Reagent. Twenty-four hours after transfection, relative firefly luciferase activity (normalized to Renilla luciferase activity) was measured using a dual-luciferase reporter gene assay system (Promega, Madison, WI, USA), and results were depicted as the percentage change over the respective control.

2.12 | Coimmunoprecipitation

Coimmunoprecipitation (co-IP) assays were carried out using Pierce crosslink immunoprecipitation kits (Cell Signaling, San Jose, CA, USA) according to the manufacturer's instructions. Cells were treated with 1 mL extraction buffer (10 mmol/L HEPES, pH 7.5, 100 mmol/L NaCl, 1 mmol/L EDTA, 10% Glycerol, 0.5% Triton X-100 and 5 μmol/L MG132). Co-IP procedures were carried out at 4°C unless otherwise indicated, using a Pierce spin column which can be capped and plugged with a bottom plug for incubation or unplugged to remove the supernatant by centrifugation at 1000 *g* for 1 minute. Binding of the first antibody to protein A/G agarose was carried out with the protocol described in Pierce crosslink immunoprecipitation kits (Thermo Scientific, Rockford, IL, USA) with slight modification. For the co-IP experiment without using disuccinimidyl suberate (DSS) cross-linking, protein A/G agarose was incubated with anti-DNMT3A antibody at 25°C for 1 hour on a mixer, followed by incubation with 600 μL precleared lysate overnight. The immunoprecipitated products were washed with washing buffer five times and eluted with 2× Laemmli buffer at 100°C for 10 minutes. The cap of the spin column was loose to avoid overpressure and leakage from the bottom when boiling. The eluting complex was subjected to SDS-PAGE separation for western blot.

2.13 | Immunohistochemistry analysis

Paraffin-embedded tissue sections on poly-L-lysine-coated slides were deparaffinized and rinsed with 10 mmol/L Tris-HCl (pH 7.4) and 150 mmol/L sodium chloride. Slides were then placed in 10 mmol/L citrate buffer (pH 6.0) at 100°C for 20 minutes in a pressurized heating chamber. Detection of antigens was carried out using incubation with the primary antibodies for 2 hours at room temperature, followed by incubation with HRP-labeled secondary antibody (MaxVision HRP-Polymer anti-Mouse/Rabbit IHC Kit, Maixin Biotech Corp, Fuzhou, China) at room temperature for 30 minutes and color development with diaminobenzidine (DAB). Digital images were acquired on an Olympus BH-2 microscope (Olympus, Tokyo, Japan) installed with a DeltaPix Camera and software (DeltaPix, Maalov, Denmark). For statistical analysis, extent (the percentage of positive cells) and intensity of staining were obtained by two pathologists. Intensity was semiquantitatively scored as weak (one point), moderate (two points), or strong (three points). For an individual case, the immunohistochemical composite score was calculated based on the extent multiplied by the intensity score.

2.14 | Statistical analysis

All experiments were carried out in triplicate at least, and each experiment was independently done at least three times. Graphical presentations were done using GraphPad Prism 5.0. Data are presented as means ± SE and were analyzed using SPSS 22.0 software (SPSS, Chicago, IL, USA). Statistical differences were tested by chi-squared test, two-tailed *t* test, one-way ANOVA test, or Fisher's exact test. Differences were considered significant at $P < .05$ (*) or highly significant at $P < .001$ (**).

3 | RESULTS

3.1 | Micro RNA-145 was inversely correlated with DNMT3A in EOC

We detected RNA levels of miR-145 and DNMT3A in 15 normal ovarian tissue samples and 31 ovarian cancer tissue samples. We found that miR-145 level in ovarian cancer tissue samples was lower than in normal ovarian tissue samples (Figure 1A), but DNMT3A level in ovarian cancer tissue samples was higher than in normal ovarian tissue samples (Figure 1C). Moreover, we found that miR-145 level was inversely associated with clinical stage (Figure 1B). By comparing the relationship between RNA expression levels of miR-145 and DNMT3A in ovarian cancer tissue samples, we found that mRNA expression of DNMT3A was negatively correlated with miR-145 in ovarian cancer tissue samples (Figure 1D). Typical immunohistochemistry (IHC) photographs from both miR-145^{high} and miR-145^{low} groups are shown in Figure 1E. We identified the differential expression of miR-145 and DNMT3A among EOC cell lines. The results showed that DNMT3A level in the miR-145 high-expression cell line (SKOV3) was lower than in the miR-145 low-expression cell line (3AO) (Figure 1F,G). Clinicopathological correlation analysis of DNMT3A level to ovarian cancer showed that overall positivity of DNMT3A was positively associated with grade of differentiation of malignant cells ($P = .036$). Although no significant differences in immunohistochemical composite score were found with differing differentiation status, the poorest differentiated tissues presented with the lowest immunohistochemical score ($P = .261$) (Table 2).

3.2 | Micro RNA-145 inhibited aerobic glycolysis by directly targeting HK2

To establish whether miR-145 was capable of inducing a metabolic shift, we examined the effect of miR-145 on glucose metabolism in human ovarian cancer cells. We found that overexpression of miR-145 (Figure 2A) inhibited glucose uptake and lactate secretion (Figure 2C) and reduced the acidity of cell culture media (Figure 2B). miR-145 mainly inhibited the expression of HK2 among other molecules implicated in the Warburg effect (Figure 2D,E). Luciferase reporter assay showed that transfection of miR-145 significantly inhibited luciferase activity in cells transfected with pGL3-HK2-wt (WT), whereas no change in luciferase activity was found in pGL3-HK2-mut (MUT) transfected cells (Figure 2F). In addition, overexpression of HK2 could counteract the inhibitory effect of overexpression of miR-145 on the Warburg effect (Figure 2G,H). Collectively, these results indicate that miR-145 inhibited aerobic glycolysis in ovarian cancer cells by targeting HK2.

3.3 | DNA methyltransferase 3A methylated pre-miR-145 and downregulated miR-145

Next, we investigated the mechanism responsible for miR-145 reduction in ovarian cancer cells. As potential methylation sites in the promoter region of miR-145 precursor genes were found using online

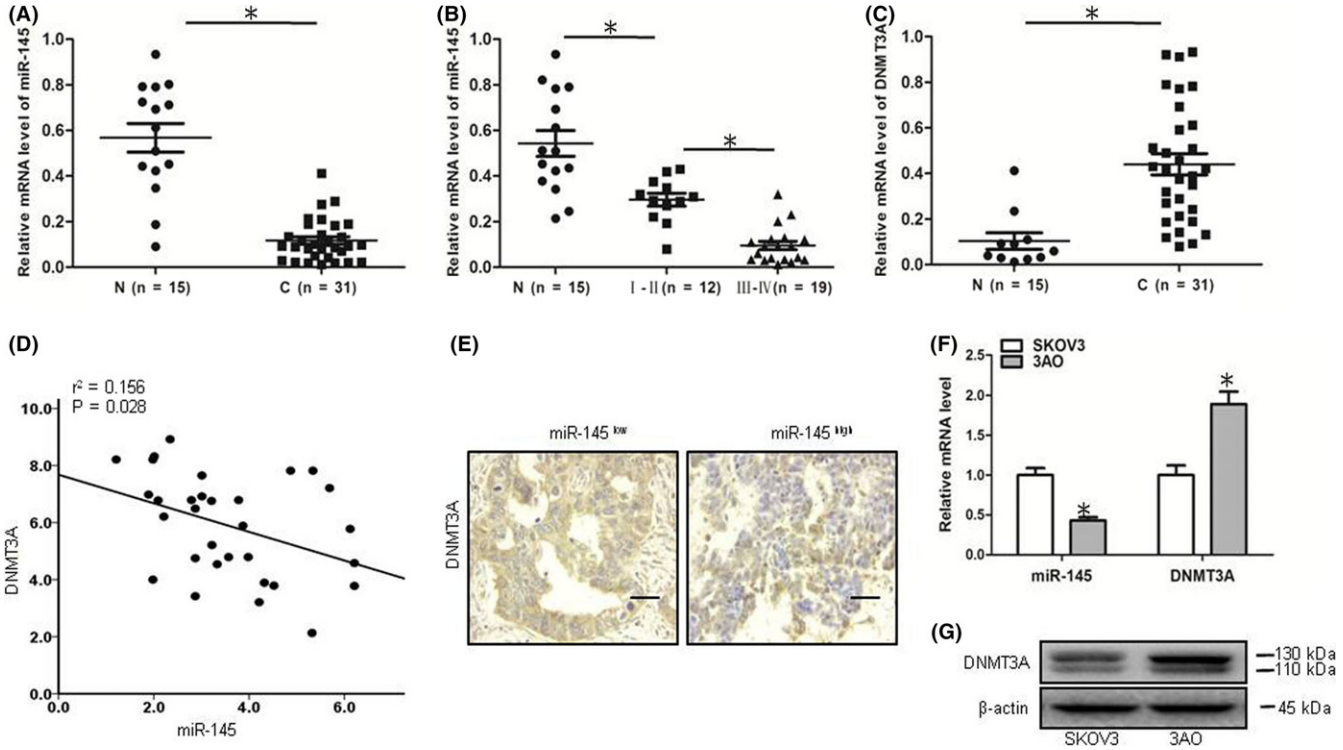

FIGURE 1 Micro RNA (miR)-145 was inversely correlated with DNA methyltransferase (DNMT)3A in epithelial ovarian cancer (EOC). A, mRNA levels of miR-145 in ovarian cancer tissue samples (n = 31) were lower than in normal ovarian tissue samples (n = 15). B, Relative expression of miR-145 in ovarian cancer tissue samples (I/II-III/IV) (n = 12/n = 19) and normal ovarian tissue samples (n = 15). C, mRNA level of DNMT3A in ovarian cancer tissue samples (n = 31) was higher than in normal ovarian tissue samples (n = 15). D, Scatter diagram showing DNMT3A expression and miR-145 expression by qPCR and their correlations (r^2 = .156, P = .028) in 31 EOC tissue samples. E, Immunohistochemistry results indicate a negative correlation between miR-145 and DNMT3A in EOC epithelia. F, Quantitative real-time PCR results show a negative correlation between DNMT3A and miR-145 in both SKOV3 and 3AO cells. G, Western blot assays show the expression of DNMT3A in SKOV3 and 3AO cells. Scale bar, 100 μm, *P < .05, t test

TABLE 2 Clinicopathological correlation of DNA methyltransferase 3A to ovarian cancer

Clinicopathological parameters of ovarian cancer	Overall positivity[a]	P value	Immunohistochemical composite scores		P value
			Mean	SD	
Age[b] (y)					
<50 (n = 12)	9 (75%)	.798	0.64	0.27	.813
≥50 (n = 19)	15 (79%)		0.63	0.43	
Grade[c]					
G1 (n = 7)	5 (71.4%)	.036*	0.62	0.38	.261
G2 (n = 10)	9 (90%)		0.82	0.43	
G3 (n = 14)	14 (100%)		0.79	0.41	

*P < .05.
[a]Percentage of cases with more than 5% positive cells.
[b]Fisher's exact test (two-tailed).
[c]t test or one-way ANOVA (two-tailed).

software (http://www.urogene.org/methprimer/), we studied the contribution of methylation regulation to the underexpression of miR-145 in EOC cells. When SKOV3 and 3AO cells were treated with the DNA methylation inhibitor 5-Aza-CdR, we found that miR-145 expression was induced up to approximately fourfold (SKOV3) or sevenfold (3AO) after 5-Aza-CdR treatment (Figure 3A).

The relationship between DNMT3A and miR-145 in EOC cells was therefore further studied. Knocking down DNMT3A (Figure 3B, D) increased the mRNA level of miR-145 (Figure 3C) and decreased the methylation levels of promoter regions in the miR-145 precursor gene (Figure 3E). Ectopic expression of DNMT3A (Figure 3F,H) repressed miR-145 (Figure 3G) and elevated methylation levels in

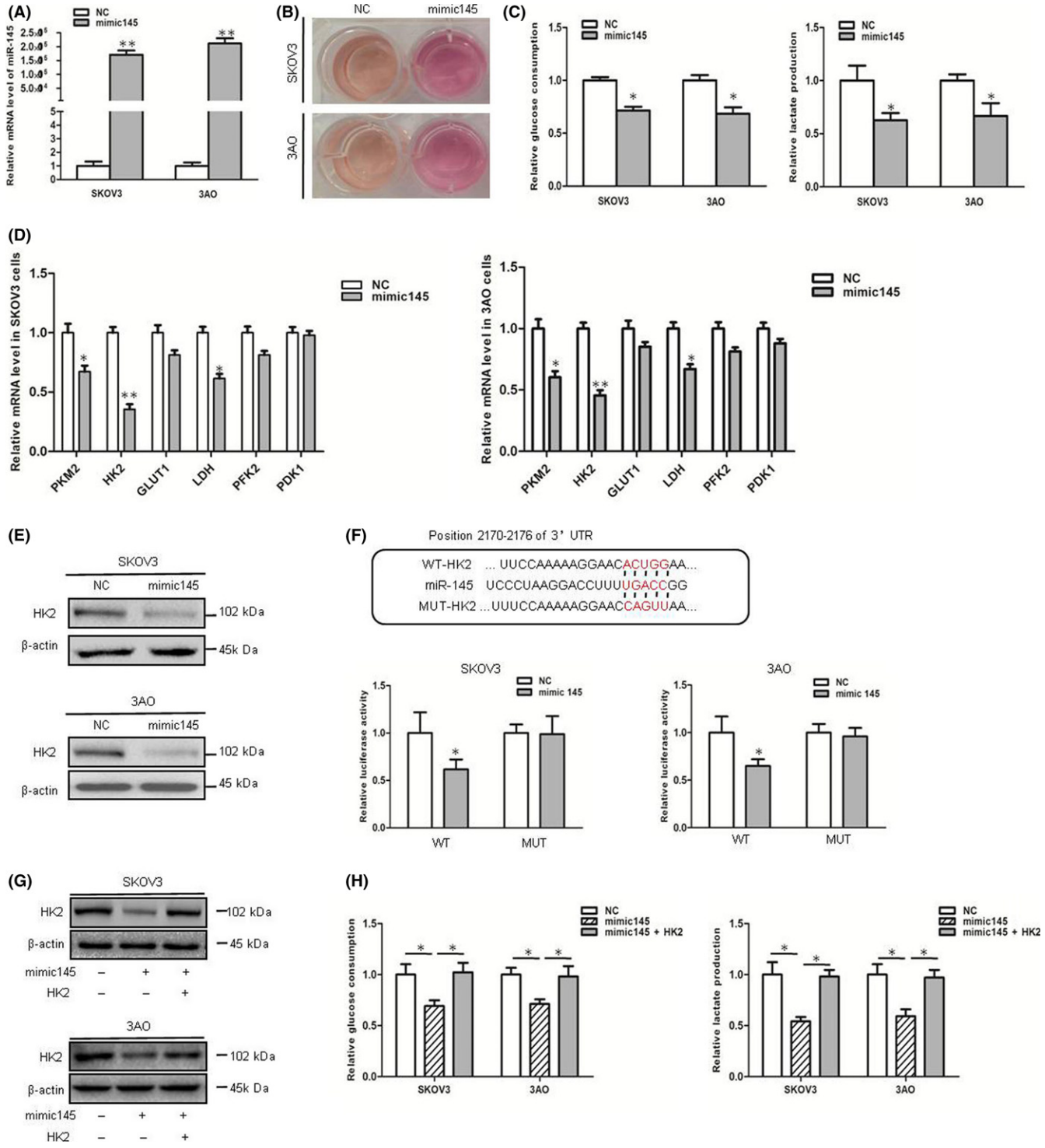

FIGURE 2 Micro RNA (miR)-145 inhibited aerobic glycolysis by directly targeting hexokinase-2 (HK2). A, Quantitative real-time PCR shows that transfection of miR-145 mimic rescued miR-145 level in SKOV3 and 3AO cells. B, SKOV3 and 3AO cells expressing either control or mimic145 were cultured for 48 h. Acidification of the culture medium was evaluated by visually inspecting the color of the medium. C, Levels of lactate in the culture medium and glucose consumption were then measured and normalized to cell number. D, Quantitative real-time PCR analysis shows that expression of metabolic enzyme genes was downregulated in SKOV3 and 3AO cells treated with mimic145 for 48 h. E, Western blot assays show that expression of HK2 was downregulated in SKOV3 and 3AO cells treated with mimic145 for 72 h. F, Luciferase reporter assays show that miR-145 targeted HK2 directly. G, Western blot assays show that overexpression of HK2 counteracted the decline of HK2 caused by miR-145 overexpression. H, Levels of lactate in the culture medium and glucose consumption were reduced by miR-145 overexpression, and the effect was attenuated by overexpression of miR-145 and HK2. $^{*}P < .05$, $^{**}P < .01$, *t* test. GLUT1, glucose transporter 1; LDH, lactate dehydrogenase; PDK1, pyruvate dehydrogenase kinase; PFK2, phosphofructokinase 2; PKM2, pyruvate kinase M2

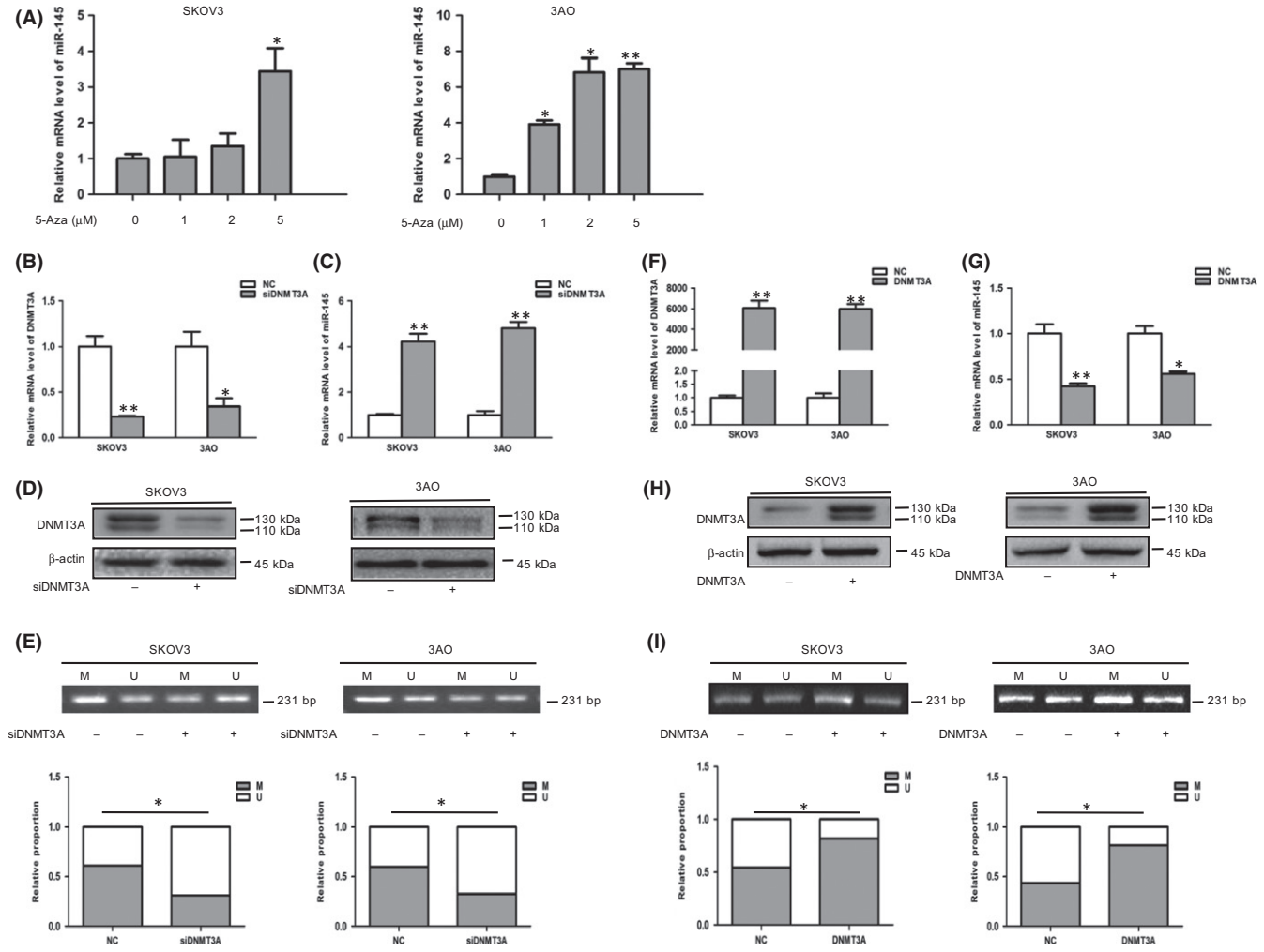

FIGURE 3 DNA methyltransferase (DNMT)3A methylated pre-micro RNA (miR)-145 and downregulated miR-145. A, Real-time PCR shows that expression of miR-145 was increased in SKOV3 and 3AO cell lines after treatment with 5-aza-2′-deoxycytidine (5-Aza-CdR) for 5 days compared with mock-treated cells. B, Quantitative real-time PCR (qRT-PCR) results show that DNMT3A mRNA level was significantly reduced by siDNMT3A transfection. C, qRT-PCR shows that knockdown of DNMT3A increased miR-145 in both SKOV3 and 3AO cells. D, Western blot assays show that knockdown of DNMT3A decreased DNMT3A expression. E, Quantitative analysis of methylation-specific PCR (MSP) results show that the methylated proportion of miR-145 precursor gene in DNMT3A siRNA-transfected cells was lower than in control cells. F, qRT-PCR results show that DNMT3A mRNA level was significantly increased by pcDNA3/Myc-DNMT3A transfection. G, qRT-PCR shows that overexpression of DNMT3A decreased miR-145 in both SKOV3 and 3AO cells. H, Western blot assays show that overexpression of DNMT3A increased DNMT3A expression. I, Quantitative analysis of MSP results show that the methylated proportion of miR-145 precursor gene in pcDNA3/Myc-DNMT3A-transfected cells was higher than in control cells. $P < .05$, $^{**}P < .01$, *t* test

the promoters of miR-145 precursor genes (Figure 3I) in EOC cells. These data demonstrate that DNMT3A downregulated miR-145 by maintaining high levels of methylation in the promoter regions of miR-145 precursor genes.

3.4 | Micro RNA-145 directly inhibited DNMT3A

We also investigated the possible effect of miR-145 on DNMT3A expression and found that overexpression of miR-145 inhibited DNMT3A expression in EOC cells (Figure 4A,B). Next, we predicted DNMT3A as a putative target gene of miR-145 by searching the TargetScan database. Luciferase reporter assay showed that transfection with miR-145 significantly inhibited the luciferase activity in cells transfected with pGL3-DNMT3A-wt (WT), whereas no change in luciferase activity was found in pGL3-DNMT3A-mut (MUT) transfected cells (Figure 4C). Collectively, these results indicate that miR-145 directly targeted DNMT3A.

3.5 | DNA methyltransferase 3A promoted the Warburg effect in EOC cells

To explore the role of epigenetic alteration of DNMT3A in tumor progression, we examined the expression levels of DNMT3A in ovarian cancer cells following treatment with 5-Aza-CdR. At baseline, high levels of DNMT3A were expressed in human ovarian cancer cells. After 4 days of 5-Aza-CdR treatment, DNMT3A expression was

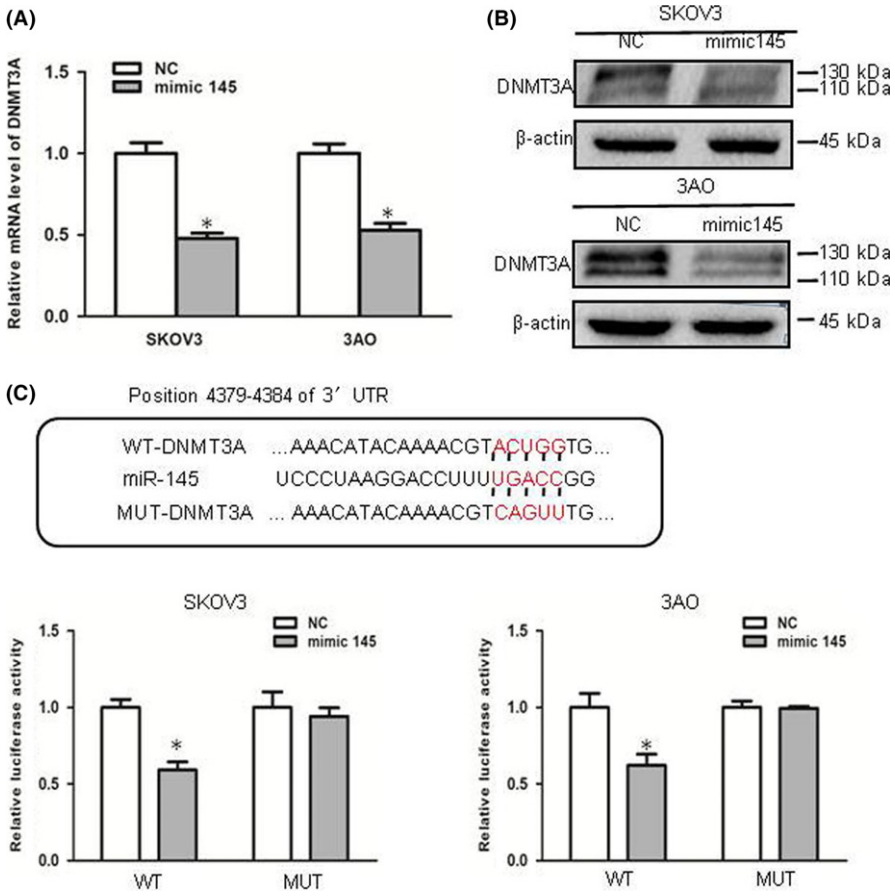

FIGURE 4 Micro RNA (miR)-145 directly inhibited DNA methyltransferase (DNMT)3A. Mimic145-mediated overexpression of miR-145 markedly repressed DNMT3A at both the mRNA and protein level in SKOV3 and 3AO cells. A, mRNA level. B, protein level. C, Luciferase reporter assays show that miR-145 targeted DNMT3A directly. *$P < .05$, *t* test

significantly decreased (Figure 5A). These findings suggest that 5-Aza-CdR alters the level of DNMT3A in ovarian cancer cells. To further determine whether reduction in DNMT3A expression regulates the Warburg effect, we examined glucose uptake and lactate secretion after 5-Aza-CdR treatment and found that reduction of DNMT3A inhibited glucose uptake and lactate secretion (Figure 5B). Reduction of DNMT3A expression mainly inhibited the expression of HK2, among other molecules implicated in the Warburg effect (Figure 5C,D, S1). Reduction of DNMT3A expression mainly inhibited the expression of HK2, among other molecules implicated in the Warburg effect (Figure 5C,D,S1). Meanwhile, overexpression of DNMT3A facilitated glucose uptake and lactate secretion (Figure 5E); DNMT3A also promoted HK2 expression (Figure 5F,G). By carrying out DNMT3A immunoprecipitation from chromatin, HK2 was coimmunoprecipitated. However, HK2 failed to be coimmunoprecipitated in DNMT3A immunoprecipitation, indicating no direct interaction between DNMT3A and HK2 (Figure 5H). Collectively, these results indicate that DNMT3A indirectly promoted aerobic glycolysis in ovarian cancer cells through HK2.

3.6 | Micro RNA-145 overexpression reversed DNMT3A-induced Warburg effect in ovarian cancer cells

As DNMT3A could induce the Warburg effect in ovarian cancer cells, and miR-145 inhibited the Warburg effect, we speculated that miR-145 might participate in the DNMT3A-triggered Warburg effect. Ectopic expression of miR-145 in DNMT3A-overexpressed cells blunted the aerobic glycolysis-inducible activity of DNMT3A, as shown by restoration of glucose uptake and lactate secretion (Figure 6A). In parallel, miR-145 recovery greatly counteracted DNMT3A-stimulated enhancement of HK2 in both SKOV3 and 3AO cells (Figure 6B,C). Taken together, these results show that miR-145 was a negative regulator of the DNMT3A-induced Warburg effect in ovarian cancer cells.

3.7 | Expression of HK2 and DNMT3A in ovarian cancer tissue subcutaneous tumors of nude mice

In preliminary studies, we found that miR-145 inhibited growth of xenografts of ovarian cancer in nude mice.[23] Here, to further investigate whether miR-145 could alter metabolism of SKOV3 cells in vivo, the subcutaneous tumors were fixed for confirmation by H&E staining and immunohistochemical analysis of HK2 and DNMT3A. As shown in Figure 7A, subcutaneous tumors in control mice showed significantly high levels of HK2 and DNMT3A. Results of western blot were consistent with immunohistochemical analysis (Figure 7B). Conversely, tumors in miR-145-up mice showed decreased HK2 and DNMT3A. These in vivo findings coincide with the in vitro changes observed in the cell models, showing that miR-145 robustly inhibited HK2 and DNMT3A expression in ovarian cancer.

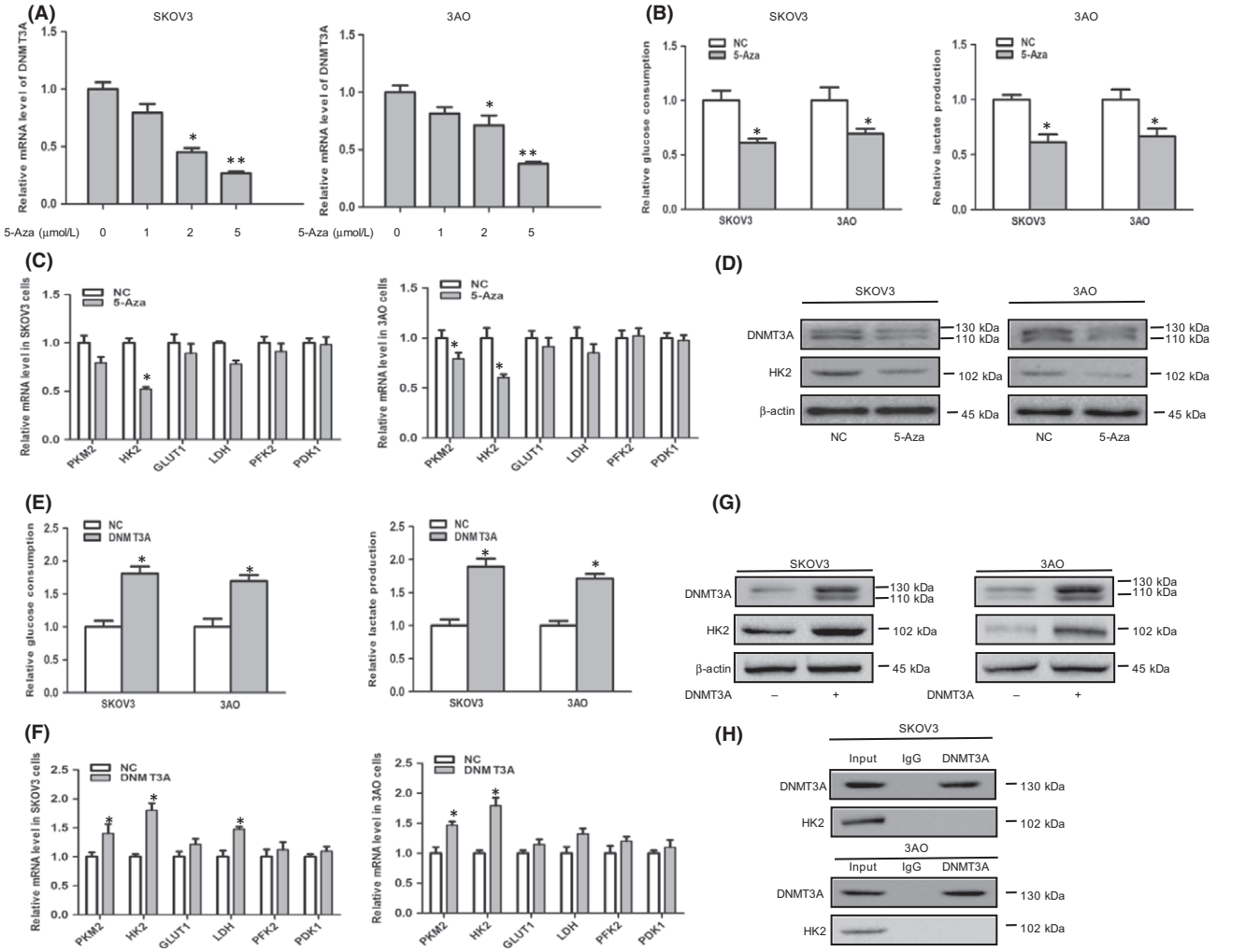

FIGURE 5 DNA methyltransferase (DNMT)3A promoted the Warburg effect in SKOV3 and 3AO ovarian cancer cells. A, DNMT3A expression was significantly decreased after 4 days of -aza-2′-deoxycytidine (5-Aza-CdR) treatment. B, Downregulation of DNMT3A by 5-Aza-CdR treatment inhibited glucose uptake and lactate secretion. C, Quantitative real-time PCR (qRT-PCR) shows that reduction of DNMT3A expression mainly inhibited the expression of HK2 among other molecules implicated in the Warburg effect. D, Western blot assays show that reduction of DNMT3A expression inhibited the expression of HK2. E, Levels of lactate in the culture medium and glucose consumption were measured and normalized to cell number. F, qRT-PCR analysis shows that expression of metabolic enzyme genes was increased in SKOV3 and 3AO cells transfected with DNMT3A expression vector for 48 h. G, Western blot assays show that expression of hexokinase-2 (HK2) was upregulated in SKOV3 and 3AO cells transfected with DNMT3A expression vector for 72 h. H, Coimmunoprecipitation assays show that there was no direct interaction between DNMT3A and HK2. $^{*}P < .05$, $^{**}P < .01$, *t* test

4 | DISCUSSION

Although DNMT3A overexpression and miR-145 silencing occur in ovarian cancer, the pathological contributions and the molecular links of these aberrations remain elusive. In our study, miR-145 silencing correlated with increased DNMT3A level, whereas miR-145 overexpression caused DNMT3A downregulation. Luciferase reporter assays confirmed that miR-145-mediated downregulation of DNMT3A occurred through direct targeting of its mRNA 3′-UTRs, whereas MSP assays found that knockdown of DNMT3A increased mRNA level of miR-145 and decreased methylation levels of promoter regions in the miR-145 precursor gene, thus suggesting a crucial crosstalk between miR-145 and DNMT3A by a double-negative feedback loop. Our data show the existence of a feedback loop between miR-145 and DNMT3A which was first related to the Warburg effect of ovarian cancer cells.

DNA methyltransferase dysregulation has frequently been reported in malignant tumors, including leukemia, prostate cancer, and gastric cancer.[24-26] We observed that treatment of SKOV3 and 3AO cells with 5-Aza-CdR resulted in increased miR-145 levels, suggesting that miR-145 expression in EOC cells might be regulated by DNA methylation. Later, overexpression of DNMT3A decreased miR-145 expression and promoted the Warburg effect. Together, these results highlight the potential therapeutic implications of DNMT3A inhibitors as well as miR-145 for future EOC treatments.

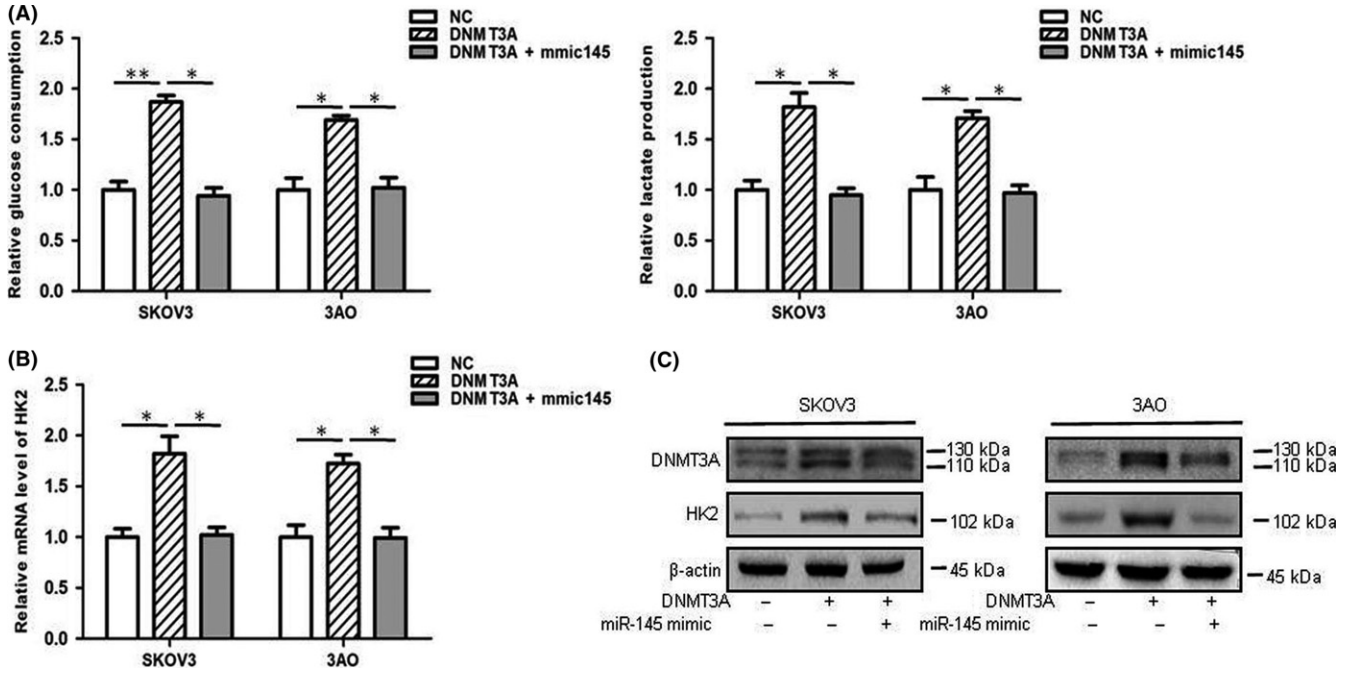

FIGURE 6 Micro RNA (miR)-145 overexpression reversed DNA methyltransferase (DNMT)3A-induced Warburg effect in ovarian cancer cells. A, SKOV3 and 3AO cells expressing negative control, overexpression of DNMT3A, and overexpression of DNMT3A plus miR-145 were cultured for 48 h. Levels of lactate in the culture medium and glucose consumption were then measured and normalized to cell number. B, Quantitative analysis and (C) western blot results indicate that HK2 increase caused by transfection with DNMT3A expression vector pcDNA3/Myc-DNMT3A was reversed by miR-145 overexpression. $^{*}P < .05$, $^{**}P < .01$, *t* test

Increasing evidence has shown that these DNMT work together to maintain a normal methylation pattern, and deregulation of either one could promote malignancies.[27] More recently, DNMT3A has been reported to participate in epithelial-mesenchymal transition (EMT).[28-30] In the present study, we showed for the first time that DNMT3A promoted the Warburg effect. Here, DNMT3A alone was found not only to increase HK2, but also to promote the expression of PKM2; glucose consumption and lactate production were accordingly promoted. DNMT3A can therefore be considered a promotor of the Warburg effect. The mediators of DNMT3A and PKM2 required identification in order to establish the functional network of DNMT3A.

Micro RNA-145 has been shown to be involved in tumor invasion and progression by targeting c-Myc, astrocyte elevated gene-1 (AEG-1), epidermal growth factor receptor (EGFR), nucleoside diphosphate linked moiety X-type motif 1 (NUDT1), and octamer-binding transcription factor 4 (OCT4) in lung adenocarcinoma (LAC)[16,31,32] and has been acknowledged as a putative tumor-suppressor miRNA. Previously, one study reported that miR-145 clustered with miR-143 to directly regulate HK-2 in renal cell carcinoma.[33] Here, miR-145 alone was found not only to repress HK2, but also to indirectly attenuate expression of PKM2 and LDH; glucose consumption and lactate production were accordingly weakened. MiR-145 can therefore be considered a repressor of the Warburg effect. In terms of the regulation of PKM2 by miR-145, as no seeding sequence of miR-145 was predicted in the 3′-UTR of the PKM2 gene, PKM2 was considered to be indirectly regulated by miR-145. In liver cancer cells, miR-145 abolished insulin-induced PKM2 expression; however, the interaction between miR-145 and PKM2 was not determined.[34] Recent studies have shown that miR-145 perturbed the Warburg effect by suppressing the pathway of KLF4/PTBP1/PKM in bladder cancer cells.[35]

The downstream mechanisms of miR-145 that alter cellular processes have been partially confirmed in several published studies. In comparison, the upstream mechanism by which miR-145 is downregulated in EOC remains less well understood. Recently, epigenetic silencing of tumor-suppressor miRNA by aberrant DNA hypermethylation has received increasing attention for a variety of cancers.[16,31,32,36] To explore the epigenetic mechanism regulating miR-145 in EOC, we compared the expression of miR-145 in SKOV3 and 3AO cell lines before and after treatment with 5-Aza-CdR. We identified that miR-145 expression was regulated by methylation. In our study, we found miR-145 inhibited the Warburg effect by targeting DNMT3A and HK2. Of note, DNMT3A did not interact with HK2. These results show that DNMT3A regulated HK2 expression by miR-145.

In a previous study, we indicated that 20(S)-Rg3 blocked EMT through DNMT3A/miR-145/FSCN1 pathways.[23] We studied the regulation of DNMT3A on EMT. In the present study, we showed for the first time that DNMT3A promoted the Warburg effect, and crucial crosstalk between miR-145 and DNMT3A by a double-negative feedback loop.

In summary, the data indicate that, with its complementary structure, miR-145 combined with and thus negatively regulated DNMT3A. DNMT3A also suppressed miR-145 through DNA methylation. The

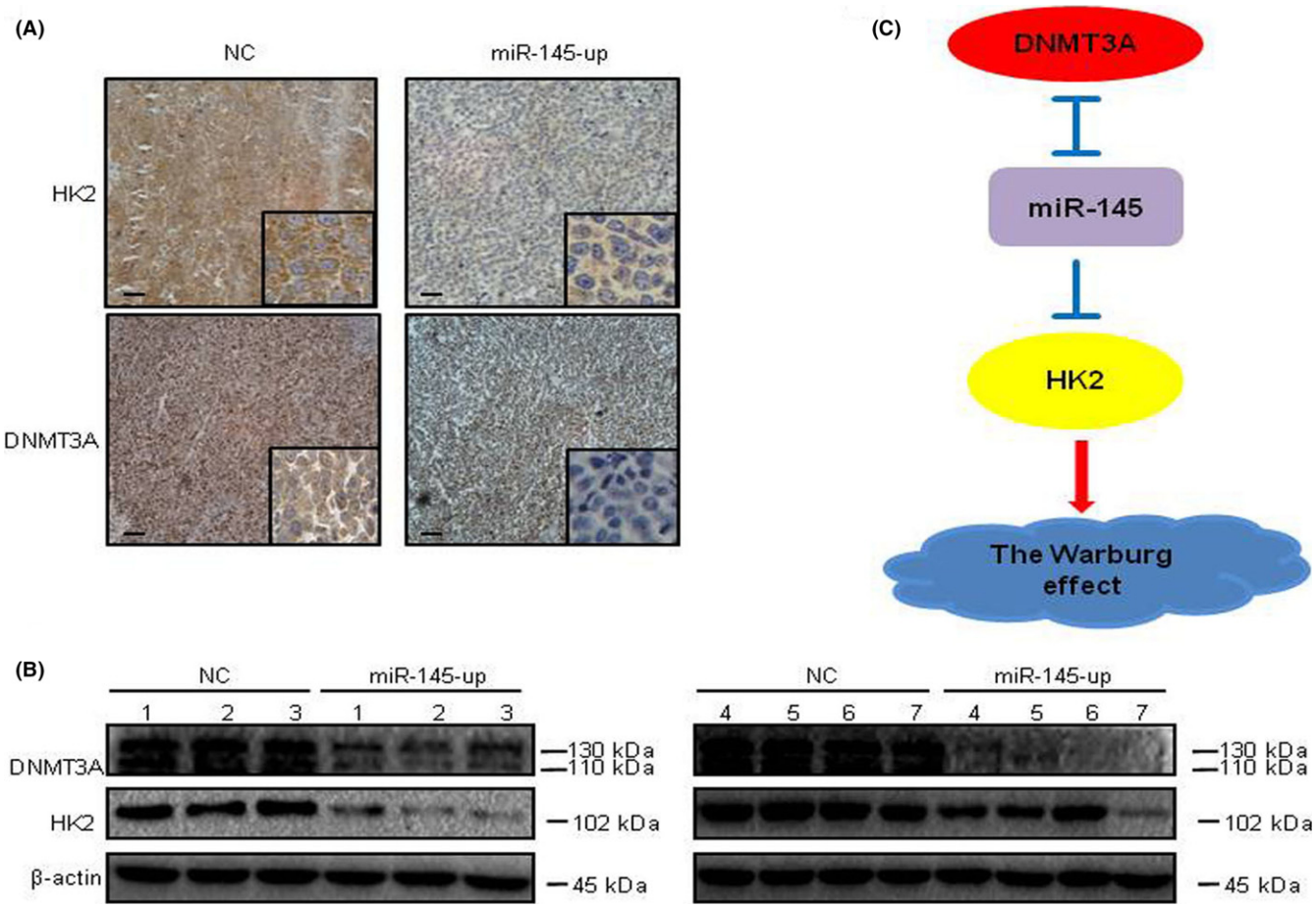

FIGURE 7 Expression of hexokinase-2 (HK2) and DNA methyltransferase (DNMT)3A in ovarian cancer tissue subcutaneous tumors of nude mice. A, Immunohistochemical staining of HK2 and DNMT3A expression in subcutaneous tumor samples (original magnification, × 100; insets, × 400). B, Western blot shows HK2 and DNMT3A expression in subcutaneous tumor samples. Numbers 1-7 represent 7 transplanted tumors in nude mice subcutaneous tumor models, respectively. C, Schematic representation of the anti-Warburg effect mechanism of DNMT3A. miR-145, micro RNA-145. Scale bar, 100 μm, $^*P < .05$, *t* test

mutual negative feedback between miR-145 and DNMT3A raises the possibility that miR-145 and DNMT3A inhibitors may be potent options for future clinical treatments of ovarian cancer.

ACKNOWLEDGMENT

This work was supported by National Natural Science Foundation of China (No. 81702577).

CONFLICTS OF INTEREST

Authors declare no conflicts of interest for this article.

ORCID

Jie Li http://orcid.org/0000-0002-4433-5393

REFERENCES

1. Cho KR, Shih Ie-M. Ovarian cancer. *Annu Rev Pathol*. 2009;4:287-313.
2. Swisher EM, Taniguchi T, Karlan BY. Molecular scores to predict ovarian cancer outcomes: a worthy goal, but not ready for prime time. *J Natl Cancer Inst*. 2012;104:642-645.
3. Lim W, Kim HS, Jeong W, et al. SERPINB3 in the chicken model of ovarian cancer: a prognostic factor for platinum resistance and survival in patients with epithelial ovarian cancer. *PLoS ONE*. 2012;7:e49869.
4. Suh DH, Kim M, Kim HJ, Lee KH, Kim JW. Major clinical research advances in gynecologic cancer in 2015. *J Gynecol Oncol*. 2016;27:e53.
5. Warburg O. On the origin of cancer cells. *Science*. 1956;123:309-314.
6. Kim JW, Dang CV. Cancer's molecular sweet tooth and the Warburg effect. *Can Res*. 2006;66:8927-8930.
7. Mathupala SP, Ko YH, Pedersen PL. Hexokinase II: cancer's double-edged sword acting as both facilitator and gatekeeper of malignancy when bound to mitochondria. *Oncogene*. 2006;25:4777-4786.
8. Jones PA, Laird PW. Cancer epigenetics comes of age. *Nat Genet*. 1999;21:163-167.
9. Baylin SB, Herman JG. DNA hypermethylation in tumorigenesis: epigenetics joins genetics. *Trends Genet*. 2000;16:168-174.
10. Gao Q, Steine EJ, Barrasa MI, et al. Deletion of the de novo DNA methyltransferase Dnmt3a promotes lung tumor progression. *Proc Natl Acad Sci USA*. 2011;108:18061-18066.
11. Bai X, Song Z, Fu Y, et al. Clinicopathological significance and prognostic value of DNA methyltransferase 1, 3a, and 3b expressions in sporadic epithelial ovarian cancer. *PLoS ONE*. 2012;7:e40024.

12. Christiansen JJ, Rajasekaran AK. Reassessing epithelial to mesenchymal transition as a prerequisite for carcinoma invasion and metastasis. *Can Res*. 2006;66:8319-8326.
13. Chan M, Liaw CS, Ji SM, et al. Identification of circulating microRNA signatures for breast cancer detection. *Clin Cancer Res*. 2013;19:4477-4487.
14. Xu Q, Liu LZ, Qian X, et al. MiR-145 directly targets p70S6K1 in cancer cells to inhibit tumor growth and angiogenesis. *Nucleic Acids Res*. 2012;40:761-774.
15. Shi B, Sepp-Lorenzino L, Prisco M, Linsley P, deAngelis T, Baserga R. Micro RNA 145 targets the insulin receptor substrate-1 and inhibits the growth of colon cancer cells. *J Biol Chem*. 2007;282:32582-32590.
16. Cho WC, Chow AS, Au JS. MiR-145 inhibits cell proliferation of human lung adenocarcinoma by targeting EGFR and NUDT1. *RNA Biol*. 2011;8:125-131.
17. Gramantieri L, Fornari F, Ferracin M, et al. MicroRNA-221 targets Bmf in hepatocellular carcinoma and correlates with tumor multifocality. *Clin Cancer Res*. 2009;15:5073-5081.
18. Kim TH, Song JY, Park H, et al. miR-145, targeting high-mobility group A2, is a powerful predictor of patient outcome in ovarian carcinoma. *Cancer Lett*. 2015;356:937-945.
19. Zhang J, Guo H, Zhang H, et al. Putative tumor suppressor miR-145 inhibits colon cancer cell growth by targeting oncogene Friend leukemia virus integration 1 gene. *Cancer*. 2011;117:86-95.
20. Sachdeva M, Zhu S, Wu F, et al. p53 represses c-Myc through induction of the tumor suppressor miR-145. *Proc Natl Acad Sci USA*. 2009;106:3207-3212.
21. Zhang J, Guo H, Qian G, et al. MiR-145, a new regulator of the DNA fragmentation factor-45 (DFF45)-mediated apoptotic network. *Mol Cancer*. 2010;9:211.
22. Sachdeva M, Mo YY. MicroRNA-145 suppresses cell invasion and metastasis by directly targeting mucin 1. *Can Res*. 2010;70:378-387.
23. Li J, Lu J, Ye Z, et al. 20(S)-Rg3 blocked epithelial-mesenchymal transition through DNMT3A/miR-145/FSCN1 in ovarian cancer. *Oncotarget*. 2017;8:53375-53386.
24. Ferreira HJ, Heyn H, Vizoso M, et al. DNMT3A mutations mediate the epigenetic reactivation of the leukemogenic factor MEIS1 in acute myeloid leukemia. *Oncogene*. 2017;36:4233.
25. Du YF, Liang L, Shi Y, et al. Multi-target siRNA based on DNMT3A/B homologous conserved region influences cell cycle and apoptosis of human prostate cancer cell line TSU-PR1. *Genet Mol Biol*. 2012;35:164-171.
26. Ding WJ, Fang JY, Chen XY, Peng YS. The expression and clinical significance of DNA methyltransferase proteins in human gastric cancer. *Dig Dis Sci*. 2008;53:2083-2089.
27. Liang G, Chan MF, Tomigahara Y, et al. Cooperativity between DNA methyltransferases in the maintenance methylation of repetitive elements. *Mol Cell Biol*. 2002;22:480-491.
28. Liu F, Zhou Y, Zhou D, et al. Whole DNA methylome profiling in lung cancer cells before and after epithelial-to-mesenchymal transition. *Diagn Pathol*. 2014;9:66.
29. Bu F, Liu X, Li J, et al. TGF-beta1 induces epigenetic silence of TIP30 to promote tumor metastasis in esophageal carcinoma. *Oncotarget*. 2015;6:2120-2133.
30. Zhou S, Li Y, Huang F, et al. Live-attenuated measles virus vaccine confers cell contact loss and apoptosis of ovarian cancer cells via ROS-induced silencing of E-cadherin by methylation. *Cancer Lett*. 2012;318:14-25.
31. Chen Z, Zeng H, Guo Y, et al. miRNA-145 inhibits non-small cell lung cancer cell proliferation by targeting c-Myc. *J Exp Clin Cancer Res*. 2010;29:151.
32. Wang M, Wang J, Deng J, Li X, Long W, Chang Y. MiR-145 acts as a metastasis suppressor by targeting metadherin in lung cancer. *Med Oncol*. 2015;32:344.
33. Yoshino H, Enokida H, Itesako T, et al. Tumor-suppressive microRNA-143/145 cluster targets hexokinase-2 in renal cell carcinoma. *Cancer Sci*. 2013;104:1567-1574.
34. Li Q, Liu X, Yin Y, et al. Insulin regulates glucose consumption and lactate production through reactive oxygen species and pyruvate kinase M2. *Oxid Med Cell Longev*. 2014;2014:504953.
35. Minami K, Taniguchi K, Sugito N, et al. MiR-145 negatively regulates Warburg effect by silencing KLF4 and PTBP1 in bladder cancer cells. *Oncotarget*. 2017;8:33064-33077.
36. Xue G, Ren Z, Chen Y, et al. A feedback regulation between miR-145 and DNA methyltransferase 3b in prostate cancer cell and their responses to irradiation. *Cancer Lett*. 2015;361:121-127.

SUPPORTING INFORMATION

Additional supporting information may be found online in the Supporting Information section at the end of the article.

How to cite this article: Zhang S, Pei M, Li Z, Li H, Liu Y, Li J. Double-negative feedback interaction between DNA methyltransferase 3A and microRNA-145 in the Warburg effect of ovarian cancer cells. *Cancer Sci*. 2018;109:2734-2745. https://doi.org/10.1111/cas.13734